Biotechnology Reports 28 (2020) e00531

Contents lists available at ScienceDirect

Biotechnology Reports

journal homepage: www.elsevier.com/locate/btre

Osthole extracted from a citrus fruit that affects apoptosis on A549 cell line by histone deacetylasese inhibition (HDACs)

Hamed A. Abosharaf[a], Thoria Diab[a], Faten M. Atlam[b], Tarek M. Mohamed[a,*]

[a] Biochemistry Division, Chemistry Department, Faculty of Science, Tanta University, Tanta, Egypt
[b] Theoretical Applied Chemistry Unit (TACO), Chemistry Department, Faculty of Science, Tanta University, Tanta, Egypt

ARTICLE INFO

Article history:
Received 8 April 2020
Received in revised form 5 August 2020
Accepted 19 September 2020

Keywords:
Osthole
Lung cancer
Histone deacetylase
Antitumor activity

ABSTRACT

This study aims to investigate the interactions between osthole extracted from Egyptian citrus fruits as HDACs inhibitor by theoretical study and practically. Besides, osthole was assed as anti-cancer activity. In this study, osthole was extracted from the Egyptian citrus fruit and was characterized. The role of osthole as in vitro inhibitor of HDACs was estimated and evaluated the antitumor activity against human lung cancer cells (A549), Caspase-9 activity was detected. The results obtained from GC–MS indicate that the grapefruit showed the highest osthole concentration compared to the other citrus fruits. Moreover, the grapefruit osthole competitively inhibits HDACs. The inhibition constant value, (Ki=3.36 mM), indicates that osthole exerts an inhibitory effect upon HDACs activity. In vitro study of osthole could inhibit the growth of A549 cells that depend on time and concentration. It also induces apoptosis and causes an increase of caspase-9 by osthole. In conclusion, grapefruit osthole could induce the apoptosis in A549 lung cancer cells by inhibiting the histone deacetylase.

1. Introduction

Cancer is considered a fatal disease that is likely to be caused mainly by environmental factors, carcinogens that can be found in surrounded food, water, air, chemicals, and sunlight to which humans are exposed. The epithelial cells cover the skin, respiratory, digestive system, and metabolized ingested carcinogen [1,2]. Based on the Egyptian National Population lung cancer is one of the most common cancers in Egypt. Lung cancer begins from the cells lining the bronchioles or alveoli. The lung cancer cells invade the lymphatic vessels that begin to grow in the lymph nodes around the bronchi and in the mediastinum (the area between the 2 lungs). When lung cancer cells reach lymphocytes, they can spread to all parts of the body's organ [3].

HDACs enzymes are acetyl group removal from the lysine residues on the N terminal of histone. HDACs have a role in gene regulation and expression by influencing the structure of compact chromatin. This causes changes in acetylation level and through it can influence the structure of chromatin compact. Thus, changes in the level of acetylation have been demonstrated by excessive gene expression in several cancer cell lines and tumor tissues. [4].

In addition to that, HDACS contains target proteins, including proteins involved in tumor development and those that control cell cycle, programmed cell death, angiogenesis, and cell invasion. Therefore, HDACS inhibitors can affect multiple cellulars on their effects and mechanisms of action including arresting cell cycle, increase apoptosis, induction of autophagy, generation of free radicals, and angiogenesis. [5,6]. Since synthetic inhibitors are toxic to patients with no specificity for some HDACS enzymes, scientists have stimulated research on natural inhibitors. [7,8]. Coumarins are natural compounds found in many plants. Osthole (7-methoxy-8-(3-methyl-2- butenyl)-2H-1-benzopyran-2-one), is also one of coumarin that first derived from Cnidium plant [9].

As reported previously, the high content of osthole is found in the mature fruit of *Cnidium monnieri*. Furthermore, some medicinal plants like *Angelica*, *Archangelica*, *Citrus*, *Fructus Cnidii,* and *Clausena* improves male function, enhance the immune system, and attenuate rheumatic disease and eliminating dampness; most of these medicinal properties are considered to attribute to bioactive components, osthole [10,11].

It has been reported that osthole has an antioxidant, anticancer, anti-inflammatory, and immunomodulatory character [9,12,13]. The current study was undertaken to look for Egyptian osthole source as a potent inhibitor for HDACs to treat the *invitro* lung cancer (A549).

Osthole inhibited the migration and invasion of MCF-7 and MDA-MB-231 cells by suppression of matrix metalloproteinases (MMP) enzyme activities [14]. Combination of osthole and

* Corresponding author.
E-mail addresses: Hamed_biochemistry@science.tanta.edu.eg (H.A. Abosharaf), thoria.diab@science.tanta.edu.eg (T. Diab), Faten.atlam@science.tanta.edu.eg (F.M. Atlam), tarek.ali@science.tanta.edu.eg (T.M. Mohamed).

https://doi.org/10.1016/j.btre.2020.e00531

platycodin D showed synergetic effect on inhibition of tumor cell proliferation and invasion of mammary carcinoma cells (MDA-MB-231 and 4T1) [15]. Osthole has been suggested to modulate PI3K/Akt signaling pathway leading to G2/M arrest and apoptosis in lung cancer A549 cells [16]. Chemically, Osthole has the potent characters to be an inhibitor for histone deacetylase as it contains a hydrophobic and aromatic group, which can act as caping agent for enzyme active site; zinc binding domain (ZBD), such ketone group or methoxy groups, which coordinates to the active site of Zn^{2+} ion.

2. Methods

2.1. Reagents

Standard osthole (M.wt = 244) and (2, 2 diphenyl-1-picrylhydrazyl) obtained from Sigma Aldrich Chemical Co. (St. Louis, Mo, U. S. A.). Caspase-9 colorimetric assay Kit and histone deacetylase colorimetric assay kit were obtained from Biovision co. (U.S.A). ANNEXIN V- FITC apoptosis detection kit was purchased from Immunostep Co. (Spain). DMEM (Dulbecco's Modified Eagle's Medium with 4.5 g/L glucose and L-glutamine), Trypsin EDTA solution, fetal bovine serum, and Penicillin-streptomycin solution were purchased from (Cambrex, bioscience. Verviers, Belgium). Grapefruit ***(Citrus paradisi)***, orange ***(Citrus sinensis),*** and lemon ***(Citrus limon (L.))*** were obtained from the local market, Tanta, Egypt.

2.2. Molecular docking software

Docking simulation was performed, **(**Molgero Virtual Docker 2008**) (**http://www.molegro.com/mvd-product.php**)** and (Thomsen and Christensen 2006) a program for conformation of ligand bind to a macromolecule.

2.3. Extraction of osthole from Egyptian citrus fruits

Osthole was extracted from three types of citrus fruits: Grapefruit (*Citrus paradisi)*, lemon (*Citrus limon*), and orange (*Citrus sinensis*) as described previously by [17] with some modifications. The raw plant materials were dried at 30 °C and finally ground to powder. Fifty grams of powdered fruits were defatted with 250 mL of petroleum ether in a Soxhlet apparatus to remove the pigments and lipids. The defatted fruits were re-extracted with 250 mL of acetone in a Soxhlet extractor for 12 h. The acetone extract was then concentrated by evaporating the solvent using a rotary evaporator under reduced pressure to get a yellow residue. The residue was dried and recrystallized in diluted ethanol (50 %), light yellow acicular crystals were obtained.

2.4. Identification of extracted osthole

The light yellow acicular crystals were blended with potassium bromide. The analysis was determined in the range between 4000 and 400 cm^{-1} at a resolution of 4 cm^{-1} using JASCO FT/IR-4100 spectrometer, Japan [18,19].

The samples were dissolved in methanol. The chemical composition of samples was performed using Trace GC DSQ II (Thermo Scientific, USA) with a direct capillary column TG–5MS (30 m x0.25 mm x0.25 μm film thickness). Osthole extracts from citrus fruits were detected and quantified according to [20], using YL9100 HPLC.

2.5. Partial purification of HDACs from rat liver

Isolation and partial purification were performed according to [21].

2.6. Determination of HDACs activity in rat liver

The activity of HDACs was determined using a colorimetric assay kit (BioVision, USA, catalog K331–100).

2.7. Kinetic inhibition of HDACs by grapefruit osthole in rat liver

Two μl of different concentrations (2–10 mM) of grapefruit osthole were added to 83 μl of the enzyme then incubated for one hour. HDACs activity was assayed as mentioned previously. The kinematic measurements (Km and Vmax) and the inhibition constant (Ki) were determined from the Lineweaver Burk plot [22].

2.8. In vitro *studies*

2.8.1. Cell culture

A human lung cancer cell line (A549) was purchased from VACSERA CO. (Giza, Egypt) and cultured according to the standard protocol for cell culture. Cells were cultured in DMEM (Dulbecco modified Eagle) having 4.5 g/L of glucose and L-glutamine and 10 % fetal bovine serum (FBS) and 1% of the penicillin-streptomycin solution. Initially, cells were seeded at a low density at 37 °C in a 5% CO_2 incubator with 95 % humidity.

2.8.2. Cell viability assay

Cell proliferation (viability) was evaluated by MTT assay according to [23].

A549 cells were counted and then re-seeded in 96-well plates to final concentration 1×10^5 cells/mL (3×10^4/well). Different concentration of grapefruit osthole extract ranged from (40.98 to 406.83 μMole) was treated in the cells. A parallel control experiment, using different concentrations of cisplatin (ranges from 6.6 to 40 μM) was run. The culture medium was removed from the 96 well microplates after 48 h of drug treatment and cells were washed twice gently by ice-cold PBS. 20 μL MTT (5 mg/mL) was added to each well. The microplate was incubated at 37 °C for 4 h in CO_2 incubator then medium/MTT was removed the 150 μl of DMSO was added to each well to dissolve the formazan produced. The microplate was incubated under shaking (at highest speed) for 15 min at 25 °C. Using a Bio-RAD microplate reader (Japan) was measured at 540 nm. The % of viability was calculated as follow:

% viability = sample absorbance/ control absorbance X 100

IC_{50} = the concentration of grapefruit osthole that inhibits 50 % of A549 cell proliferation.

2.8.3. Determination of caspase-9 activity

The determination of caspase-9 activity was detected by using the Caspase-9 Colorimetric Assay Kit *(BioVision, USA, cat.no. K119)* [24].

Two million cells were cultivated in a 12-well plate for 24 h. Cells were treated with grapefruit osthole with different concentration from 94.26 to 377 μM for 24, 48 h [24]. Cells were suspended in 50 μl of lysis buffer and incubated for 10 min. Cells were centrifuged for 1 min. The supernatant (cytosolic extract) was transferred to a fresh tube. Fifty μl of 2X buffer was added to each sample5 μl of the 4 mM LEHD-*p*NA substrate was added and incubated at 37 °C for 2 h. The absorbance was detected at 400 nm using Bio-RAD microplate reader (Japan).

2.8.4. Apoptosis analysis by flow cytometry

Measurement of apoptosis was performed using ANNEXIN V-FITC APOPTOSIS DETECTION KIT (*Immunostep, Spain*) [25].

Two million cells were cultured in T-25 culture flask for 24 h. Cells were treated with osthole extract with different concentrations from94.26 to 377 μMole. The culture medium was removed from flasks after 48 to 72 h and cells were washed gently

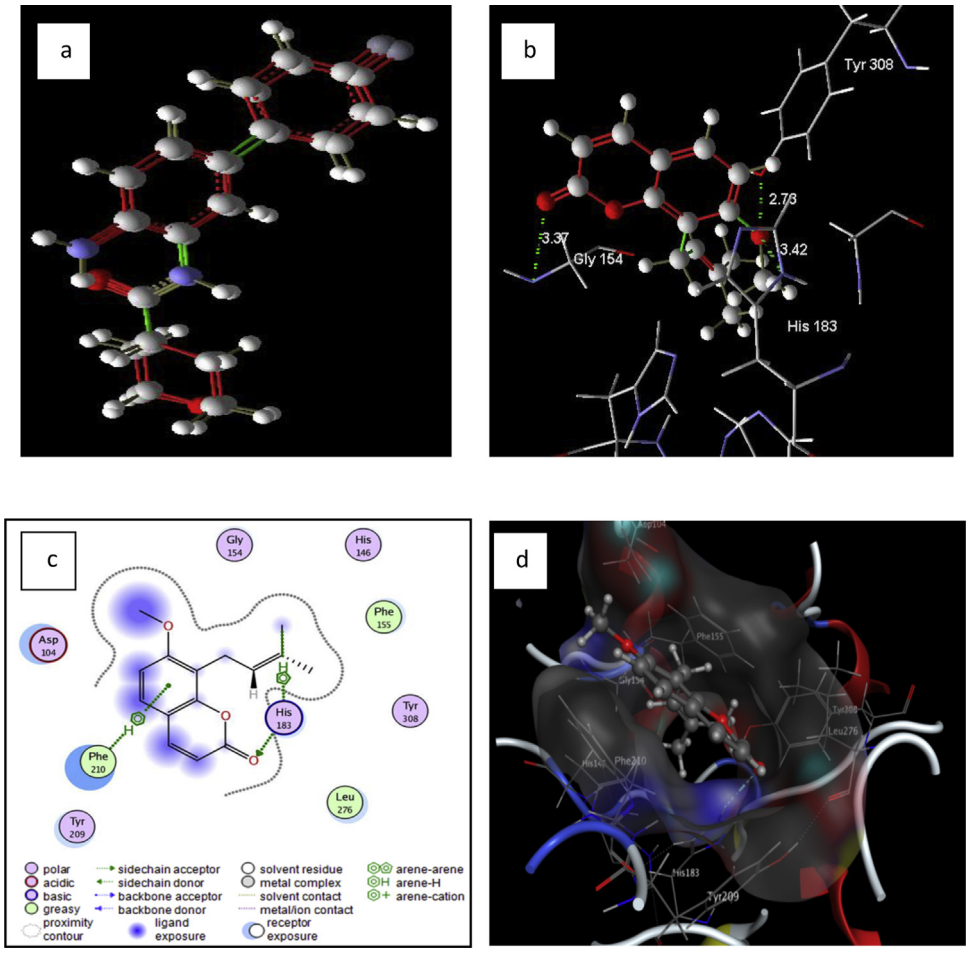

Fig. 1. **(a)** Superimposition of the native ligand found within the crystal structure and the redocked pose of the same ligand**. (b)** Binding of osthole to the active site of HDAC-like protein. Hydrogen bond interactions are indicated by dotted lines, with numerals indicating **the** distance in angstroms, protein is represented by sticks, and osthole is represented by balls and sticks. **(c)** Surface representation of the hydrophobic interaction of osthole with an active pocket of HDAC-like protein**. (d)** 3D model of the interaction between osthole with an active pocket of HDAC-like protein's active site. The protein is represented by molecular surface and osthole is depicted by balls and sticks.

twice with ice-cold PBS, and resuspended in 1X Annexin-binding buffer.at a concentration 1×10^6cells/mL. Five μl of the Annexin V-FITC and 5 μl of PI were added to each 100 μl of cell suspension. The cells were incubated for 15 min at room temperature (25 °C) in the dark. Then, 400 μl of 1X Annexin-binding buffer was added. Samples were analyzed by flow cytometry (Beckman coulter, U.S. A.) within one hour.

2.8.5. Statistical analysis

The data were showed and analysed by using Excel Microsoft office and Graphpad prism followed by one way ANOVA follower by post hoc Ducan's multiple range tests were done to evaluate the relative HDC activity with different concentration of osthol treatment. Finally, the data presented as Mean ± SD of repeated experiments.

3. Results

3.1. Molecular docking analysis of osthole with HDAC- like protein

The optimum molecular structure of the inhibitor was known by some experiments from semi-empirical calculations and conformational search. The native ligand has been removed from the active site and then was docked into the binding site of its enzyme to characterize the binding pocket of HDAC-like protein (the grid dimensions were: x = 67.71 Å, y=30.78 Å and z = 2.52 Å, with a grid spacing of 9 Å). The docked orientations with a root mean square deviation between the predicted conformer and the observed X-ray crystallographic conformer, 0.320 Å, were clustered together (superimposition) as shown in Fig. 1(a).

Docking calculations of osthole showed has 3H-bond interactions with the important amino acid residues, Tyr308, Gly154, and His183, with H-bond distances 2.73, 3.37 and 3.42 Å, respectively, (Fig. 1: b). This could explain the inhibition efficiency of osthole.

Also, the docking calculations showed that the phenolic moiety and the methyl group of osthole are close to Phe210 and His183 residues, respectively. The van der Waals forces were found responsible for the affinity of osthole with HDAC-like protein (Fig. 1: c). The surface representation of the minimum energy structure of the complex of osthole docked in the active site of the HDAC-like protein is shown from the molecular modeling study (Fig. 1: d). The calculated parameters of osthole molecule of molecular docking calculations are shown in **(**Table 1**).**

3.2. Identification of extract osthole

Osthole was extracted from three different citrus fruits by the method described previously. The osthole structure was identified using the FTIR spectrum and GC–MS.

FTIR spectrum showed a carbonyl (C=O) peak at 1747 and 1649 cm^{-1}, CO— stretching peak at 1048 and 1049 cm^{-1} and aromatic

Table 1
The calculated parameters, binding interaction (BE), Inhibition constant (Ki), molecular docking score (MDS), Rerank score (RS), Hydrogen bond interaction energy (HB), obtained from the molecular docking calculations.

Parameter	BE	Ki	MDS	RS	HB
Inhibitor (Osthole)	6.9	3E-6	−106.233	−77.136	−0.779

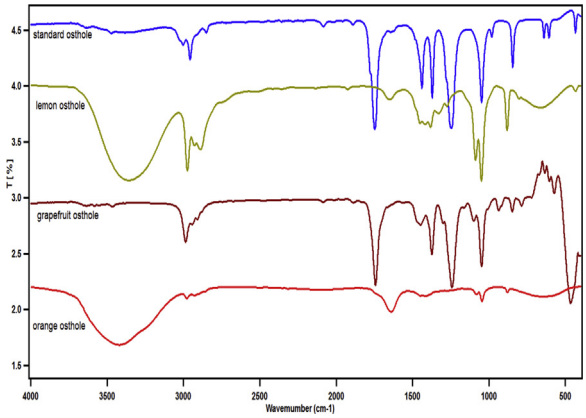

Fig. 2. FTIR of extracted osthole from different citrus fruits compared to standard.

CC= peak at 1439 and 1451 cm^{-1}. These data confirm the skeleton of osthole in citrus fruits compared to standard as shown in (Fig. 2).

Further evidence of the examined compound was obtained from GC–MS that showed well-separated peaks with retention time 16.56 identical to the osthole standard solution. The molecular weight of osthole was 244 in grapefruit and lemon. Moreover, the appearance of the ion peak at 213 *m/z* is due to the cleavage of a methoxy moiety from the molecule. These data proposed the structure of osthole, with $C_{15}H_{16}O_3$ molecular formula and confirmed the presence of osthole in grapefruit and lemon only as shown in (Fig. 3).

Moreover, HPLC analysis indicated the presence of osthole in grapefruit and lemon with concentrations 8.6 and 0.286 mg/g dry weight, respectively. The chromatogram of standard osthole (Fig. 4, panel A), grapefruit osthole (Fig. 4, Panel B) and lemon osthole (Fig. 4, panel C) showed that osthole had retention time 6.5, 6.8 and 6, respectively.

3.3. Partial purification of HDACs

HDACs were partially purified from rat liver as shown in (Table 2). HDACs was purified about 4-fold starting from the crude homogenate to the final step. The 45 % ammonium sulfate fractionation yield was 111.76 units. The ammonium sulfate fraction retained approximately 27 % of the original activity (yield). The pellet of 25 % and 45 % ammonium sulfate had specific activities of 3.41 and 7.61 unit/mg protein, respectively. Also, the total protein content was estimated for each step giving 3.8, and 14.68 mg, respectively.

3.4. Kinetic inhibition of rat liver HDACs with grapefruit osthole

The activity of HDACs was detected in the presence of different grapefruit osthole concentrations ranged from 2 to10 mM. As illustrated in (Fig. 5), the enzyme was inhibited by grapefruit osthole in a concentration-dependent manner. Grapefruit osthole was inhibited 50 % of HDACs at a concentration of 8.6 mMole. According to Lineweaver Burk plot, different concentrations of grapefruit osthole (4.3, 6, and 8.6 μMole) showed an inhibition pattern in which the lines intersected at the Y-axis. The K_m of the enzyme acetylated poly lysin was changed (increased) and the V_{max} value was unchanged (Fig. 6: A). Accordingly, the type of inhibition is competitive. The inhibition constant, K_i value was found to be 3.36 mM. (Fig. 6: B).

3.5. Effect of grapefruit on A549 cell proliferation

A549 cell proliferation was determined by using MTT assay and compared with cisplatin as a positive control. The results showed that the viability of A549 cells significantly decreased by increasing grapefruit osthole concentrations with IC_{50} 188.5 μMole (Fig. 7). HDAC activity was slightly inhibited in A549 cells treated with grapefruit osthole for 24 h compared to the untreated cells. When the cells were incubated with grapefruit osthole for 48 and 72 h, HDAC activity was significant ($p < 0.01$) decreased depending on increasing time and dose concentration as shown in (Fig. 8).

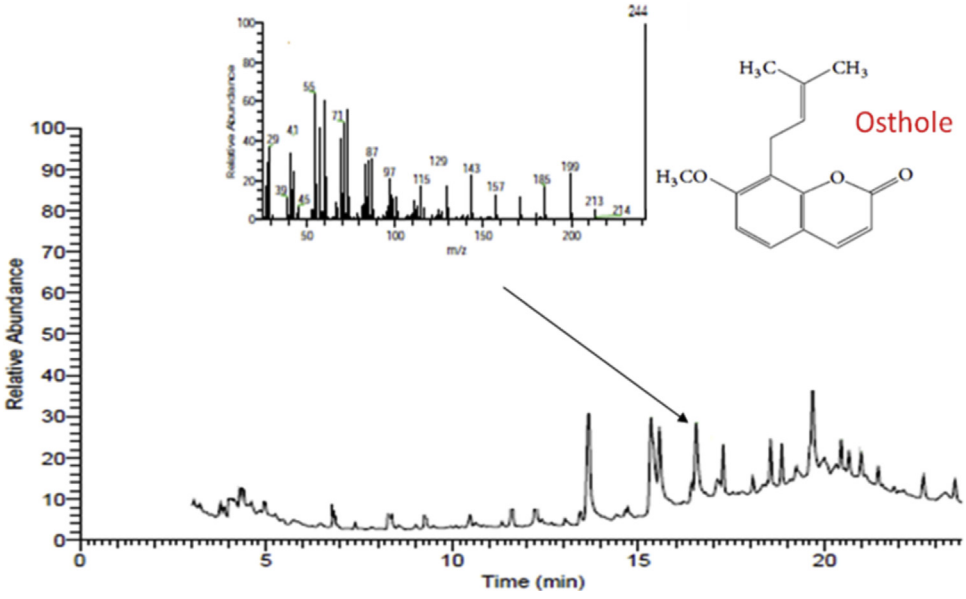

Fig. 3. GC–MS chromatogram of grapefruit osthole extract. The arrow shows the peak of osthole.

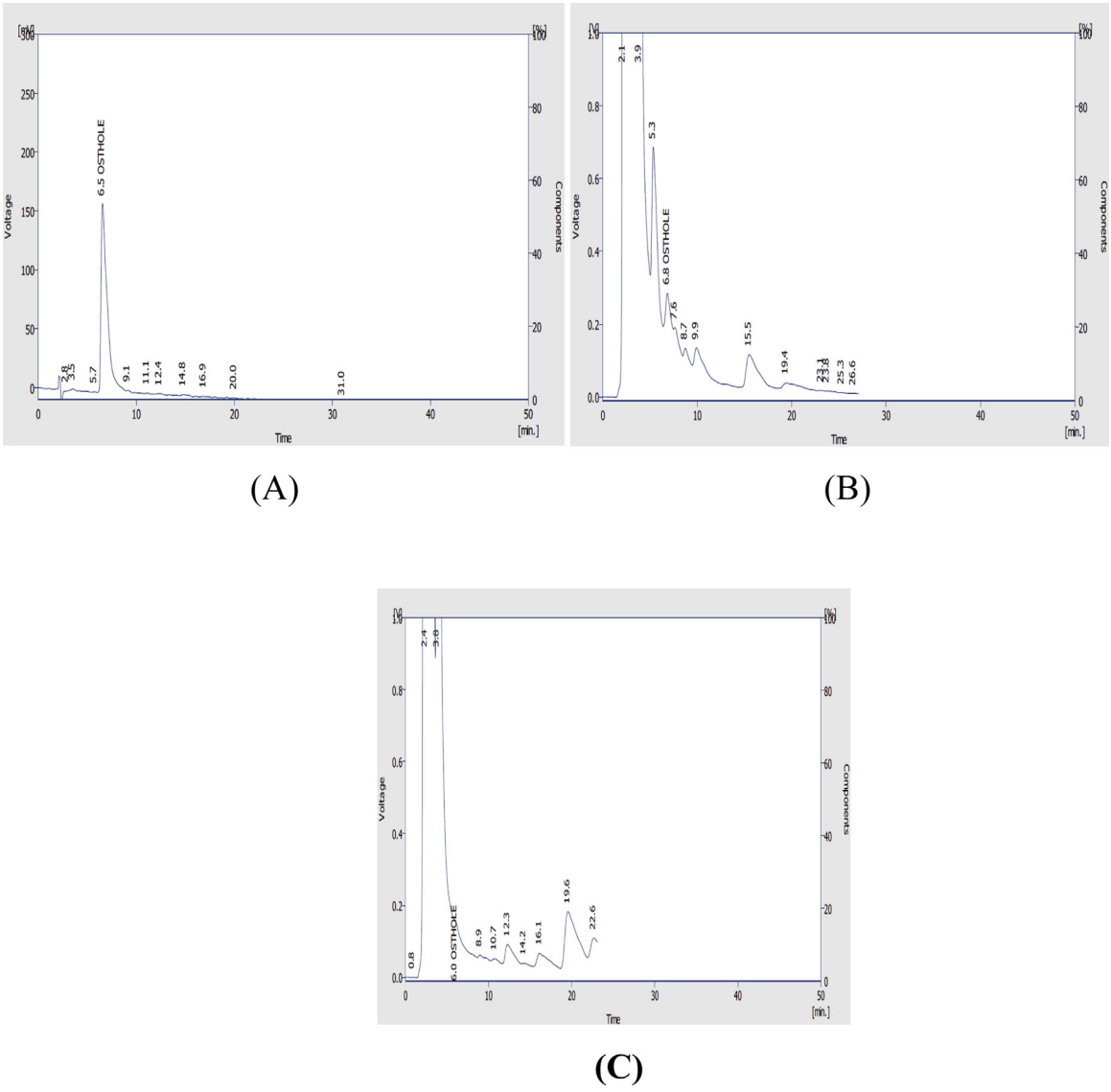

Fig. 4. HPLC chromatogram of standard osthole (A), osthole extracted from grapefruit (B), and osthole extracted from lemon (C).

Table 2
: Purification scheme of HDACs from rat liver.

Step	Total Protein conc.(mg)	Total HDACs activity (μmol/min)	Specific activity (unit/ mg protein)	Yield (%)	fold1
Crude	194	414.3	2.14	100	1
pellet of 25 % amm.sulfate	3.8	12.94	3.41	3.12	1.59
pellet of 45 % amm.sulfate	14.68	111.76	7.61	26.98	3.55

3.6. Effect of grapefruit osthole on Caspase-9 activity

The effect of grapefruit osthole on A549 cells caspase-9 activity was determined and compared with cisplatin as a positive control. Caspase-9 activity was increased in A549 cells treated with different concentrations (Fig. 9).

3.7. Apoptotic effect of grapefruit osthole

Flow cytometry analysis measured treatment of different concentrations of grapefruit osthole to A549 cells for 48 h (Fig. 4A, B). Compared to the control group the numbers of early and late apoptotic cells were significantly increased. The proportion of early and late apoptotic cells in the 188.5 μM treatment cells were about thirteen times higher than in cells free drug. The apoptosis treated cells were increased as a dose-dependent manner (Fig. 10).

4. Discussion

Regulating HDACS activity is very important for the epigenetic regulation of gene expression by studying its effects on the compact chromatin structure. Work by [26] revealed that the

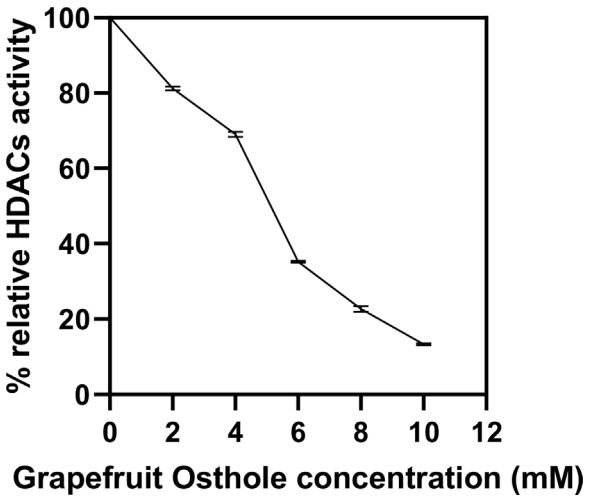

Fig. 5. Inhibition of HDACs' activity by grapefruit osthole in rat liver. The data were expressed as mean ± SD of triplicate experiments.

alterations level of acetylation and overexpression of HDACs have been detected in various cancer cell lines and tumor tissues. Consequently, this enzyme is an interesting target for the searching of antiproliferative drugs and it is not surprising that numerous approaches to the design of new antitumor agents were based on the search for HDACs inhibitors. It has been reported that many HDACS synthetic inhibitors have cytotoxic effects. These inhibitors have undesirable side effects associated with some chemotherapy drugs. In this manner, we increase the demand for novel anti-tumor drugs with low side effects. New insights are required to find potential natural inhibitors of HDACs may avoid such side effects [27,28].

Osthole, a naturally occurring compound, has a variety of pharmacological and biochemical uses that have potential therapeutic applications. It found mainly in 14 species of Umbelliferae family and 17 of the Rutaceae family [9]. One of the aims of this work was to show the effect of osthole on HDACs. To achieve this purpose, molecular docking studies were performed. Based on the results of molecular docking, it has been found that osthole showed favorable binding with HDAC-like protein.

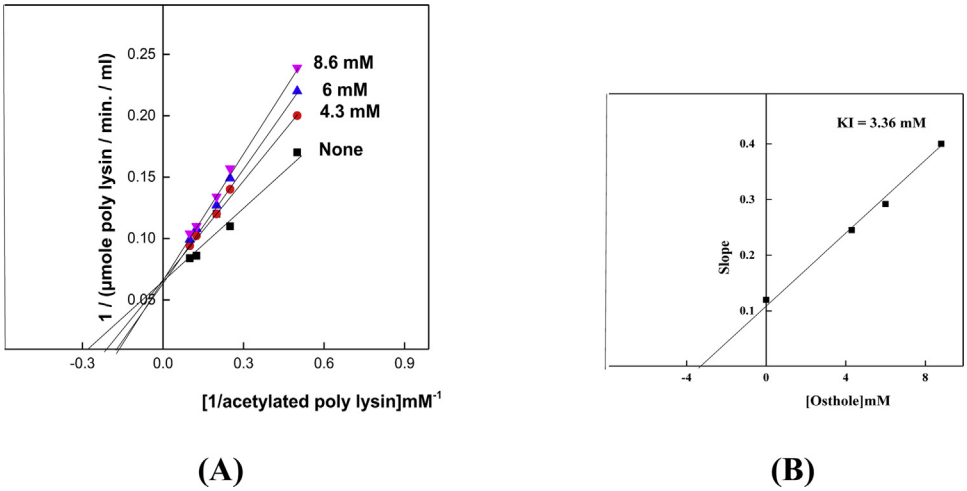

Fig. 6. Inhibition study of rat liver HDACs (A), and Inhibition constant (K_i) (B) with grapefruit osthole.

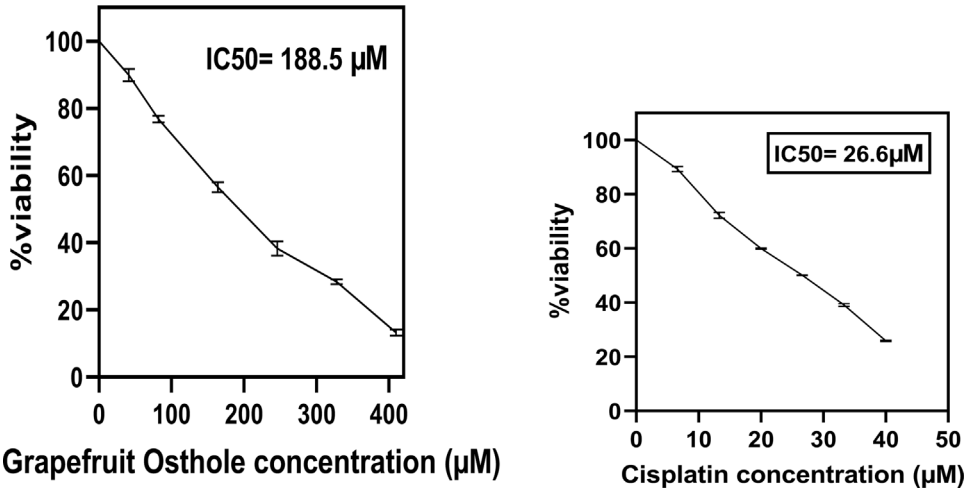

Fig. 7. Effect of grapefruit osthole and cisplatin on A549 cell viability by the MTT assay. The data were expressed as Mean ± SD of separated triplicate experiments. The data were expressed as Mean ± SD of triplicated experiments.

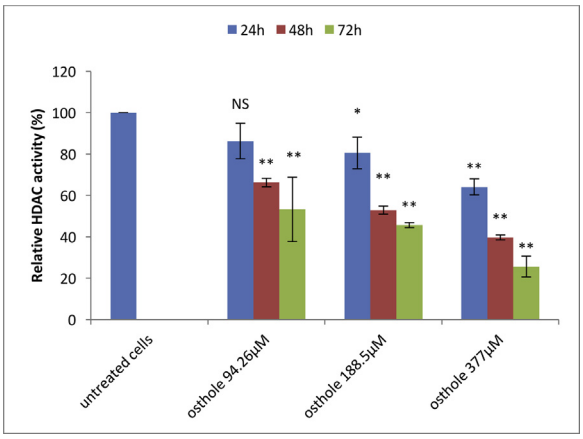

Fig. 8. Effect of grapefruit osthole on HDAC activity in A549 cells after 24, 48 and 72 h treatment with different concentrations of grapefruit osthole. The data were expressed as Mean ± SD of triplicated experiments, Graphpad prism used to determine the significany, where * $p < 0.05$, ** $p < 0.01$ compared to untreated cells.

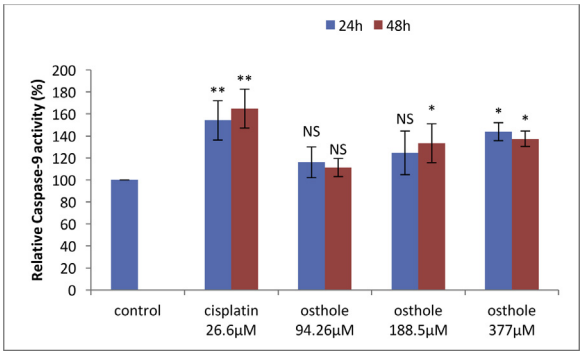

Fig. 9. Effect of grapefruit osthole on caspase-9 activity in A549 cells after 24 and 48 h treatment with different concentrations of grapefruit osthole. The data were expressed as Mean ± SD of triplicated experiments, Graphpad prism used to determine the significany,where * $p < 0.05$, ** $p < 0.01$ compared to control.

Osthole was extracted from Egyptian citrus fruits including grapefruit, lemon, and orange. The structure of osthole was confirmed using different methods.

FTIR revealed that the presence of coumarinic carbonyl peak at 1747 cm^{-1}, CO— stretching peak at 1048 cm^{-1} and aromatic CC peak at 1600 $cm^{-=1}$, confirms the skeleton of osthole in citrus fruits. This is in agreement with that previously described by [19] who suggested the presence of coumarinic carbonyl peak at 1721 cm^{-1} and C=C peak at 1606 cm^{-1} of osthole extracted from Persian *cinidium monnieri*. In another study, osthole was extracted from *prangos genus*, showed the presence of coumarinic carbonyl peak at 1717 cm^{-1} and C=C peak at 1604 cm^{-1} [18].

Further evidence of the examined extracts was obtained from the GC–MS analysis which confirmed the FTIR data. The GC–MS analysis showed well-separated peaks with retention time 16.56 identical to the osthole standard solution with molecular weight 244 in grapefruit and lemon. Besides, the appearance of the ion peak at *m/z* 213 is due to the cleavage of a methoxy moiety from the molecule. The obtained data is inconsistent with the proposed structure of the known osthole with $C_{15}H_{16}O_3$ molecular formula and confirmed the presence of osthole in tested citrus fruits except orange. These results are the same with obtained by [29].

The concentration of osthole in grapefruit and lemon extracts was determined by the HPLC. The concentrations of osthole in grapefruit and lemon were found to be 8.6 and 0.286 mg/g dry weights, respectively. The obtained data illusterated that the concentrations of osthole were higher than those obtained by [29] in which the concentrations of osthole in the peel of grapefruit and lemon were 12 and 7 μg/g dry weights, respectively. Another study reported that the concentration of osthole was found to be 20 mg/g powdered *Cnidium monnieri* fruit, which is considered to be the main source of osthole [30]. Our results might have a commercial application by finding a promising and cheap local source of osthole.

To compare the theoretical data obtained by the molecular docking with the experimental data, HDACs were isolated from rat liver and assayed in the presence and absence of grapefruit osthole. The rat liver HDACs' activity was inhibited by grapefruit osthole. The inhibition showed a direct interaction between the enzyme and the grapefruit osthole with IC_{50} 8.6 mM of grapefruit osthole, whereas the results obtained by [31] suggested that the IC_{50} value of apigenin which is considered to be a natural inhibitor of HDACs was 32 mM.

The grapefruit osthole acts as a competitive inhibitor with the K_i value is 3.36 mM. This value is consistent with that obtained by molecular docking indicating that there is resonable aspect between the laboratory and theoretical data. Moreover, our result agrees with [32,33] in which Hela cell HDACs were inhibited by 2, pyrrolidinone-n butyric acid, topiramate, valproic acid and butyric acid with K_i 2.25, 2.22 and 0.51 mM, respectively. On another hand, the inhibition of butyric acid of HDACs was carried with K_i 60 mM [34].

Taken together, we demonstrate that osthole extracted from Egyptian grapefruit may act as a natural inhibitor for HDACs. This was supported by theoretical data provided by molecular docking as well as practical experiments.

Consequently, we evaluated the cytotoxic effect of grapefruit osthole against A549 lung cell line by MTT assay. The IC_{50} of grapefruit osthole in the cell line was 188.5 μM after 48 h of treatment. On the other hand, the IC_{50} of cisplatin, which was used as a reference drug, was 26.6 μM after 48 h of treatment. In parallel, the activity of HDAC was assayed in the tested cell line at different time points (24, 48, and 72 h) and the data showed that the enzyme activity decreased by 19.4 %, 47.1 %, and 54.5 %, respectively upon treatment with 188.5 μM of osthole. These findings are consistent with those previously obtained by [16].

The effect of osthole inhibitor on HDC is due to the hydrophobic nature of this inhibitor. This hydrophobicity is corresponded with the chemical feature of the capping group in known HDAC inhibitors that form hydrophobic contact with the surface residues at the edge of the active site [35]. This result was confirmed by our molecular docking by using EA DOCK software.

In order to investigate the apoptosis-inducing potentials of the grapefruit osthole, the caspase-9 activity was detected. The results showed that caspase-9 activity was increased by (16, 24, and 43 %) compared to control after 24 h of treatment with grapefruit osthole. After 48 h of osthole treating, the activity of caspase-9 still elevated but slightly lower than that from at 24 h.

This is in agreement with that described by [36] who studied the effect of cinidium osthole on human carcinoma cell lines. They found that osthole could increase caspase-8 and -9 in H1299, PC3, and SKNMC cells. Osthole induces apoptosis in these cell lines through both intrinsic and extrinsic pathway. In addition, [1,2] studied the effect of osthole on human breast cancer cell lines. They found that osthole induced apoptosis through increasing the activity of caspase-9 and caspase-3.

Consequently, flow cytometric analysis was used to discriminate between viable and apoptotic lung cancer cells after treatment. Egyptian grapefruit osthole induced apoptosis in lung cancer cells. We found that (4, 16, and 20 %) of cells in early apoptosis and (12.8, 27.4, and 46.3 %) of cells in late apoptosis. However, apoptotic cells increased with increas**ing** time to 72 h (5,

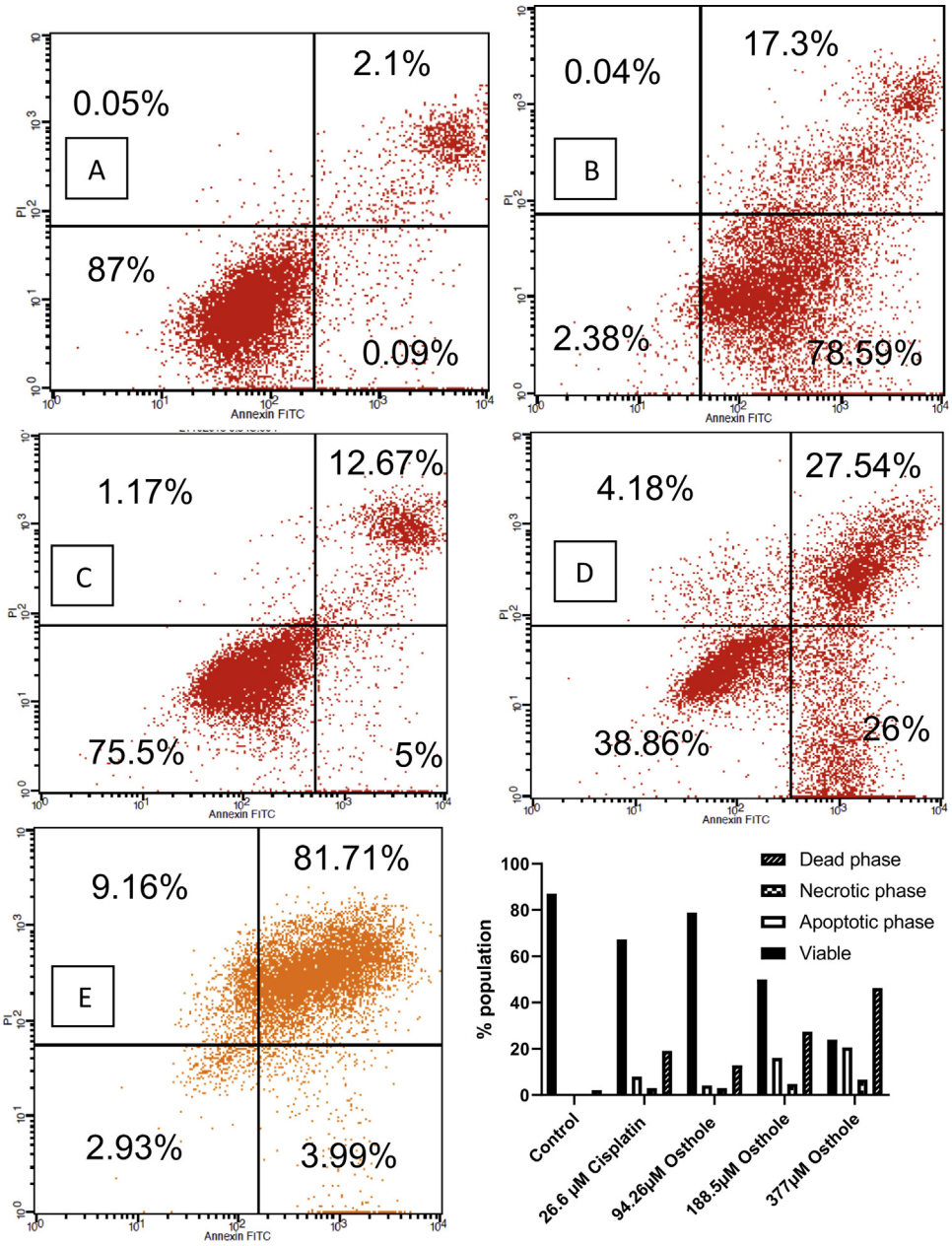

Fig. 10. Flow cytometric analysis of A549 cells treated with grapefruit osthole. Plots show Annexin V-FITC and propidium iodide stained A549 cells untreated (panel A) and treated (for 72 h) with cisplatin, 94.26, 188.5, and 377 μM of grapefruit osthole (panels B, C, D, and E, respectively).

26, and 4 %) in early apoptosis and (12.6, 27.5, and 81.7 %) of cells in late apoptosis.

In the previous studies, [16] studied the effect of osthole on the human lung cancer A549 cells and their results showed that 150μM of osthole induced about 17 % of cell in early apoptosis and about 20 % of cells in late apoptosis. The authors have attributed such findings to the role of osthole in the induction of G2/M arrest and apoptosis possibly by down-regulating Akt signaling in the investigated cell line. Moreover, [1,2] studied the effects of osthole on human breast cancer cells MDA-MB 435 for proliferation, cell cycle, and apoptosis. Their results showed that upon treating with 100 μM of osthole for 36 h, the apoptosis increased to 45 %.

These observations suggest that osthole may have an anti-cancer effect through inhibition of HDAC, which is involved in many pathways in cancer treatment such as activation of tumor suppressor gene (p53), cyclin-dependent kinase inhibitor (p21) and down-regulation of cyclin A correlated well with the decreased cyclin-dependent kinase 2 (Cdk2) activity leading to apoptosis and cell cycle arrest [37]. Therefore, it appears that apoptosis induced by increasing caspase 9 activity occurred via an intrinsic pathway in A549 cells.

In conclusion, the grapefruit osthole act as a natural inhibitor of HDACs with Ki 3.36 mM. Moreover, it considers a valuable therapeutic agent for lung cancer treatment. Further *in vivo* studies could confirm this data in the future.

Authors statements

Mr/ Hamed Adel
Biochemistry division, Chemistry Department, Faculty of Science, Tanta University, Tanta, Egypt.
Dr/Thoria Diab
Biochemistry division, Chemistry Department, Faculty of Science, Tanta University, Tanta, Egypt.

Dr/Faten Atlam
Theoretical Applied Chemistry Unit (TACO), Chemistry Department, Faculty of Science, Tanta University, Tanta, Egypt
Prof/ Tarek Mohamed (corresponding author)
Biochemistry division, Chemistry Department, Faculty of Science, Tanta University, Tanta, Egypt

Declaration of Competing Interest

The authors report no declarations of interest

Acknowledgment

Thanks to the Chemistry department, Faculty of Science, Mansoura University where GC–MS analysis was carried out. Special thanks to Prof. Dr. Adel Selim, professor of Organic Chemistry, Chemistry Department, Faculty of Science, Tanta University for his valuable help in the analysis of GC–MS data.

Appendix A. Supplementary data

Supplementary material related to this article can be found, in the online version, at doi:https://doi.org/10.1016/j.btre.2020.e00531.

References

[1] L. Wang, Y. Peng, K. Shi, H. Wang, J. Lu, Y. Li, C. Ma, Osthole inhibits proliferation of human breast cancer cells by inducing cell cycle arrest and apoptosis, J. Biomed. Res. 29 (2) (2015) 132–138.
[2] L. Wang, Y. Peng, K. Shi, H. Wang, J. Lu, Y. Li, C. Ma, Osthole inhibits proliferation of human breast cancer cells by inducing cell cycle arrest and apoptosis, J. Biomed. Res. 29 (2) (2015) 132.
[3] A.S. Ibrahim, H.M. Khaled, N.N. Mikhail, H. Baraka, H. Kamel, Cancer incidence in Egypt: results of the national population-based cancer registry program, J. Cancer Epidemiol. 2014 (2014).
[4] J.E. Bolden, M.J. Peart, R.W. Johnstone, Anticancer activities of histone deacetylase inhibitors, Nat. Rev. Drug Discov. 5 (9) (2006) 769–784.
[5] M. Mottamal, S. Zheng, T.L. Huang, G. Wang, Histone deacetylase inhibitors in clinical studies as templates for new anticancer agents, Molecules 20 (3) (2015) 3898–3941.
[6] M. Mrakovcic, J. Kleinheinz, L.F. Fröhlich, p53 at the crossroads between different types of HDAC inhibitor-mediated cancer cell death, Int. J. Mol. Sci. 20 (10) (2019) 2415.
[7] M. Jung, Inhibitors of histone deacetylase as new anticancer agents, Curr. Med. Chem. 8 (12) (2001) 1505–1511.
[8] A.K. Singh, A. Bishayee, A.K. Pandey, Targeting histone deacetylases with natural and synthetic agents: an emerging anticancer strategy, Nutrients 10 (6) (2018) 731.
[9] L. You, S. Feng, R. An, X. Wang, Osthole: a promising lead compound for drug discovery from a traditional Chinese medicine (TCM), Nat. Prod. Commun. 4 (2) (2009) 297–302.
[10] Z.W. Zhou, P.X. Liu, [Progress in study of chemical constituents and anti-tumor activities of Cnidium monnieri], Zhongguo Zhong Yao Za Zhi 30 (17) (2005) 1309–1313.
[11] A. Jarzab, J. Luszczki, M. Guz, K. Skalicka-Wozniak, M. Halasa, J. Smok-Kalwat, K. Polberg, A. Stepulak, Combination of osthole and cisplatin against rhabdomyosarcoma TE671 cells yielded additive pharmacologic interaction by means of isobolographic analysis, Anticancer Res. 38 (1) (2018) 205–210.
[12] J.R. Hoult, M. Paya, Pharmacological and biochemical actions of simple coumarins: natural products with therapeutic potential, Gen. Pharmacol. 27 (4) (1996) 713–722.
[13] R. Wang, J. Kong, D. Wang, L.L. Lien, E.J. Lien, A survey of Chinese herbal ingredients with liver protection activities, Chin. Med. 2 (2007) 5.
[14] D. Yang, T. Gu, T. Wang, Q. Tang, C. Ma, Effects of osthole on migration and invasion in breast cancer cells, Biosci. Biotechnol. Biochem. 74 (7) (2010) 1430–1434.
[15] Y. Ye, X. Han, B. Guo, Z. Sun, S. Liu, Combination treatment with platycodin D and osthole inhibits cell proliferation and invasion in mammary carcinoma cell lines, Environ. Toxicol. Pharmacol. 36 (1) (2013) 115–124.
[16] X. Xu, Y. Zhang, D. Qu, T. Jiang, S. Li, Osthole induces G2/M arrest and apoptosis in lung cancer A549 cells by modulating PI3K/Akt pathway, J. Exp. Clin. Cancer Res. 30 (1) (2011) 33.
[17] M. Zimecki, J. Artym, W. Cisowski, I. Mazol, M. Wlodarczyk, M. Glensk, Immunomodulatory and anti-inflammatory activity of selected osthole derivatives, Z. Naturforsch. C 64 (5–6) (2009) 361–368.
[18] S. Sajjadi, H. Zeinvand, Y. Shokoohinia, Isolation and Identification of Osthol From the Fruits and Essential Oil Composition of the Leaves of Prangos Asperula Boiss 2009: 5, (2009) .
[19] H.-K. Liu, Y.-K. Lo, T.-R. Tsai, T.-M. Cham, Physicochemical Characterizations of Osthole-hydroxypropyl-?-cyclodextrin Inclusion Complexes with High-Pressure Homogenization Method, J. Food Drug Anal. 18 (6) (2010).
[20] Y. Li, F. Meng, Z. Xiong, H. Liu, F. Li, HPLC determination and pharmacokinetics of osthole in rat plasma after oral administration of Fructus Cnidii extract, J. Chromatogr. Sci. 43 (8) (2005) 426–429.
[21] B. Heltweg, M. Jung, A homogeneous nonisotopic histone deacetylase activity assay, J. Biomol. Screen. 8 (1) (2003) 89–95.
[22] H. Lineweaver, D. Burk, The determination of enzyme dissociation constants, J. Am. Chem. Soc. 56 (3) (1934) 658–666.
[23] F. Denizot, R. Lang, Rapid colorimetric assay for cell growth and survival. Modifications to the tetrazolium dye procedure giving improved sensitivity and reliability, J. Immunol. Methods 89 (2) (1986) 271–277.
[24] P.L. Kuo, Y.L. Hsu, C.H. Chang, C.C. Lin, The mechanism of ellipticine-induced apoptosis and cell cycle arrest in human breast MCF-7 cancer cells, Cancer Lett. 223 (2) (2005) 293–301.
[25] G. Koopman, C.P. Reutelingsperger, G.A. Kuijten, R.M. Keehnen, S.T. Pals, M.H. van Oers, Annexin V for flow cytometric detection of phosphatidylserine expression on B cells undergoing apoptosis, Blood 84 (5) (1994) 1415–1420.
[26] H. Zheng, W. Zhao, C. Yan, C.C. Watson, M. Massengill, M. Xie, C. Massengill, D. R. Noyes, G.V. Martinez, R. Afzal, Z. Chen, X. Ren, S.J. Antonia, E.B. Haura, B. Ruffell, A.A. Beg, HDAC inhibitors enhance T-Cell chemokine expression and augment response to PD-1 immunotherapy in lung adenocarcinoma, Clin. Cancer Res. 22 (16) (2016) 4119–4132.
[27] M.L. Neuhouser, Dietary flavonoids and cancer risk: evidence from human population studies, Nutr. Cancer 50 (1) (2004) 1–7.
[28] A.L. Demain, P. Vaishnav, Natural products for cancer chemotherapy, Microb. Biotechnol. 4 (6) (2011) 687–699.
[29] I. Al-Doush, T. Mahier, M. Al Tufail, M. Bogusz, Occurrence of Osthole in commonly available citrus fruits analyzed with GC-MS and LC-QTOF-MS, International Journal of Applied Research in Natural Products 5 (4) (2012) 37–43.
[30] Q. Chen, P. Li, F. Yuan, F. Cheng, J. He, J. Liu, Z. Zhang, Identification and quantification of the volatile constituents in Cnidium monnieri using supercritical fluid extraction followed by GC-MS, J. Sep. Sci. 32 (2) (2009) 252–257.
[31] M. Pandey, P. Kaur, S. Shukla, A. Abbas, P. Fu, S. Gupta, Plant flavone apigenin inhibits HDAC and remodels chromatin to induce growth arrest and apoptosis in human prostate cancer cells: in vitro and in vivo study, Mol. Carcinog. 51 (12) (2012) 952–962.
[32] P.A. Marks, R.A. Rifkind, V.M. Richon, R. Breslow, T. Miller, W.K. Kelly, Histone deacetylases and cancer: causes and therapies, Nat. Rev. Cancer 1 (3) (2001) 194.
[33] S. Eyal, B. Yagen, E. Sobol, Y. Altschuler, M. Shmuel, M. Bialer, The activity of antiepileptic drugs as histone deacetylase inhibitors, Epilepsia 45 (7) (2004) 737–744.
[34] L.S. Cousens, D. Gallwitz, B.M. Alberts, Different accessibilities in chromatin to histone acetylase, J. Biol. Chem. 254 (5) (1979) 1716–1723.
[35] W.J. Huang, C.C. Chen, S.W. Chao, S.S. Lee, F.L. Hsu, Y.L. Lu, M.F. Hung, C.I. Chang, Synthesis of N-Hydroxycinnamides capped with a naturally occurring moiety as inhibitors of histone deacetylase, ChemMedChem 5 (4) (2010) 598–607.
[36] Y. Shokoohinia, L. Hosseinzadeh, M. Alipour, A. Mostafaie, H.-R. Mohammadi-Motlagh, Comparative evaluation of cytotoxic and apoptogenic effects of several coumarins on human cancer cell lines: osthole induces apoptosis in p53-deficient H1299 cells, Adv. Pharmacol. Sci. 2014 (2014).
[37] Y.-C. Yang, C.-N. Chen, C.-I. Wu, W.-J. Huang, T.-Y. Kuo, M.-C. Kuan, T.-H. Tsai, J.-S. Huang, C.-Y. Huang, NBM-TL-BMX-OS01, semisynthesized from osthole, is a novel inhibitor of histone deacetylase and enhances learning and memory in rats, Evid. Based Complement. Altern. Med. 2013 (2013).